nature materials

REVIEW ARTICLE

PUBLISHED ONLINE: 23 NOVEMBER 2010 | DOI: 10.1038/NMAT2898

# A ten-year perspective on dilute magnetic semiconductors and oxides

Tomasz Dietl[1,2]*

**Over the past ten years, the search for compounds combining the properties of semiconductors and ferromagnets has evolved into an important field of materials science. This endeavour has been fuelled by many demonstrations of remarkable low-temperature functionalities in the ferromagnetic structures (Ga,Mn)As and p-(Cd,Mn)Te, and related compounds, and by the theoretical prediction that magnetically doped, p-type nitride and oxide semiconductors might support ferromagnetism mediated by valence-band holes to above room temperature. Indeed, ferromagnetic signatures persisting at high temperatures have been detected in a number of non-metallic systems, even under conditions in which the presence of spin ordering was not originally anticipated. Here I review recent experimental and theoretical developments, emphasizing that they not only disentangle many controversies and puzzles accumulated over the past decade but also offer new research prospects.**

Advances in the epitaxy of semiconductor compounds have made it possible to fabricate quantum structures in which confined electrons or photons have remarkable properties and functionalities. Similarly, the atomic precision of metal and oxide film deposition has allowed us to master a number of striking spin transport phenomena. The discovery of ferromagnetism in p-type Mn-doped IV–VI (ref. 1), III–V (refs 2–4) and II–VI (refs 5, 6) compounds has led to the development of multifunctional materials systems that combine the capabilities of semiconductor quantum structures and ferromagnetic multilayers, and has enabled the study of collective magnetic phenomena as a function of the spin and carrier densities.

Over the past ten years or so, the field of ferromagnetism in dilute magnetic semiconductors (DMSs) and dilute magnetic oxides (DMOs) has developed into an important branch of materials science. The comprehensive research on these systems has been stimulated by a succession of demonstrations of outstanding low-temperature functionalities in (Ga,Mn)As, p-(Cd,Mn)Te and related structures[7,8], some examples being spin injection[9], the control of magnetism by means of electric fields[10,11] and electric currents[12], tunnelling anisotropic magnetoresistance in planar junctions[13] and in the Coulomb blockade regime[14], and current-induced domain displacement without the assistance of a magnetic field[15]. These findings have brought into focus the interplay of magnetization texture and dynamics with carrier population and currents, which is a broad topic of current research on spintronic materials. In parallel with this, since the first report on $(Ti,Co)O_2$ (ref. 16), the persistence of spontaneous magnetization to above room temperature has been found in a number of DMOs and DMSs, and even for materials nominally containing no transition-metal impurities.

However, despite the many investigations, the origin and control of ferromagnetism in DMSs and DMOs is, arguably, the most controversial research topic in materials science and condensed-matter physics today. As I will emphasize, the abundance of contradicting views has resulted from intertwined theoretical and experimental challenges requiring the application of cutting-edge computational and materials nano-characterization methods that are often becoming available only now. In this way, DMSs and DMOs emerge as outstanding systems in which to test our understanding of unanticipated relationships between growth conditions and self-organized alloy structure[17] and among quantum localization, carrier correlation and ferromagnetism, and are thus an area of active research[18–20].

I begin this review by recalling the foundations of the *p–d* Zener model, which was proposed by myself and colleagues a decade ago to describe the origin and properties of ferromagnetism in p-type Mn-doped semiconductors[21]. A crucial role of Anderson–Mott localization in the physics of these systems is then discussed in the context of other models put forward to explain remarkable findings on (Ga,Mn)As that have accumulated over recent years. I show that the *p–d* Zener model describes a number of thermodynamic and micromagnetic properties of III–V and II–VI DMSs and continues to be a good starting point from which to consider research on hole-mediated ferromagnetic semiconductors. The second part of the review is devoted to the origin and control of high-temperature ferromagnetism in DMSs and DMOs. I argue, using the results of much work on nano-characterization, that puzzling properties of these compounds reflect the presence of a highly non-random distribution of magnetic cations therein. Although a number of appealing functionalities have already been demonstrated for these ferromagnetic–semiconductor nanocomposites, we are only beginning to demonstrate the device structures of these emerging materials systems.

## *p–d* Zener model

In view of the progress in materials fabrication by epitaxial methods[2–6,22], it was timely a decade ago to understand the ferromagnetism in DMSs and to ask whether the Curie temperature, $T_C$, can be raised to more than 300 K from the 110 K observed at that time in (Ga,Mn)As containing only 5% Mn (ref. 22). Photoemission[23] and optical studies in the single-impurity limit[24] demonstrated that Mn provides both localized spins and itinerant holes mutually coupled by a *p–d* exchange interaction. Zener[25] first proposed the model of ferromagnetism driven by the exchange interaction between band carriers and localized spins. In the case of semiconductors, the Zener model[26,27] is equivalent to the approach developed by Ruderman, Kittel, Kasuya and Yosida, in which the Friedel oscillations of the spin density are taken into account[26].

In the proposed implementation of the Zener model, the structure of the valence subbands was described by the Kohn–Luttinger

[1]Institute of Physics, Polish Academy of Sciences, Aleja Lotników 32/46, PL-02-668 Warszawa, Poland, [2]Institute of Theoretical Physics, University of Warsaw, PL-00-681 Warszawa, Poland. *e-mail: dietl@ifpan.edu.pl

six-band k·p Hamiltonian, taking the spin–orbit interaction into account[21]. Thermodynamic characteristics were then evaluated in the mean-field approximation. At the same time, arguments were presented as to why the model is valid even on the insulator side of the Anderson–Mott metal-to-insulator transition (MIT), provided that the holes remain weakly localized. This approach was found to constitute an appropriate minimal theory, capable of adequately describing the magnitudes of $T_C$ and the magnetic anisotropy fields induced by biaxial strains in (Ga,Mn)As and p-(Zn,Mn)Te (ref. 21). It was also pointed out that GaN and ZnO containing appropriately high concentrations of both Mn spins ($x \gtrsim 5\%$) and delocalized or weakly localized holes in the valence band ($p \gtrsim 3.5 \times 10^{20}$ cm$^{-3}$) might support ferromagnetic order to above room temperature. It was emphasized, however, that before this prediction can be verified, important issues of solubility limits and self-compensation, and of the transition to a strong-coupling case with decreasing lattice constant, need to be addressed experimentally[21].

## Guide through other models

Extensive studies during the past decade have made it clear that ferromagnetic DMSs and DMOs form two distinct classes. The first class comprises p-type Mn-based semiconductors, in which the ferromagnetism is associated with the presence of holes. Here, step-by-step improvements in growth protocols and in post-growth processing have made it possible to increase the Mn and hole densities, particularly in (Ge,Mn)Te (ref. 28) and (Ga,Mn)As (refs 29–31), in which the respective Curie temperatures now approach 190 K at a value of the effective Mn concentration, $x_{eff}$, less than 10%, as implied by the saturation magnetization (Fig. 1). Although this evolution of $T_C$ is consistent with the $p$–$d$ Zener model, its basic foundation, namely that in the concentration range relevant to ferromagnetism the holes reside in the valence band in (Ga,Mn)As and related systems, is objected to by two schools of thought.

First, following pioneering *ab initio* work carried out on (In,Mn)As (ref. 32) it has been argued, on the basis of the outcome of available first-principles methods, that the holes reside in band-gap states derived from the transition-metal $d$ levels in this case, the relevant spin–spin coupling mechanism would be the double exchange[33,34]. Second, a series of findings from optical and transport studies, being hard to reconcile with expectations for holes moving in a weakly perturbed valence band, have been taken as evidence for the location of the Fermi energy within a Mn-acceptor impurity band. Here the relevant states have been assumed to be either detached from the valence band or to retain the $d$ character of Mn dopants even in the region where they overlap with the valence band on the metallic side of the MIT[35,36].

To another class of ferromagnetic systems belongs a broad range of semiconductors, oxides and carbon derivatives that have ferromagnetic-like features persisting to above room temperature without the presence of itinerant holes or, in some cases, even without intentional doping by transition-metal impurities[37–39]. Four different models have been proposed to explain the origin of this intriguingly robust ferromagnetism.

First, in a long series of *ab initio* works a ferromagnetic ground state has been found for dilute transition-metal spins even in the absence of band carriers[40]. After pioneering work[32,41], the effect has been assigned to the ferromagnetic superexchange[41] or, more frequently, double exchange[32] that arises, within the computation methodologies used, if the states derived from the transition-metal $d$ levels are partly occupied for one spin direction[40]. In the second model, it is supposed that electrons either residing in the conduction band[42] or forming bound magnetic polarons[43] mediate ferromagnetic couplings between dilute transition-metal spins. Alternatively, the presence of these couplings is assigned to carriers residing on defects, such as vacancies[44], or on residual impurities, such as hydrogen[45]. In the third explanation, the ferromagnetic response is related to spins of electrons that reside on point or extended defects and are coupled by an exchange interaction. Within this so-called $d^0$ model of high-temperature ferromagnetism, the presence of magnetic impurities is either unnecessary or serves merely to bring the Fermi level to the relevant defect states[46]. Finally, it has been persistently suggested[39,47] that the limited solubility of transition-metal impurities in particular hosts may result in the formation of nanoscale regions containing a large density of magnetic cations and thus specified by a high spin-ordering temperature.

## Where do the holes reside in (Ga,Mn)As?

According to the double-exchange scenario[33,34], the anticrossing picture[36,48,49] and the impurity-band models[4,35], the hole states retain impurity-band characteristics in the density regime relevant to the ferromagnetism of (Ga,Mn)As. For a comprehensive presentation of arguments in favour of such a scenario, I refer the reader to ref. 35.

Another view, shared by me and presented in detail elsewhere[50,51], is that similarly to other doped semiconductors, in p-type DMSs the carrier localization results from a collective effect of randomly

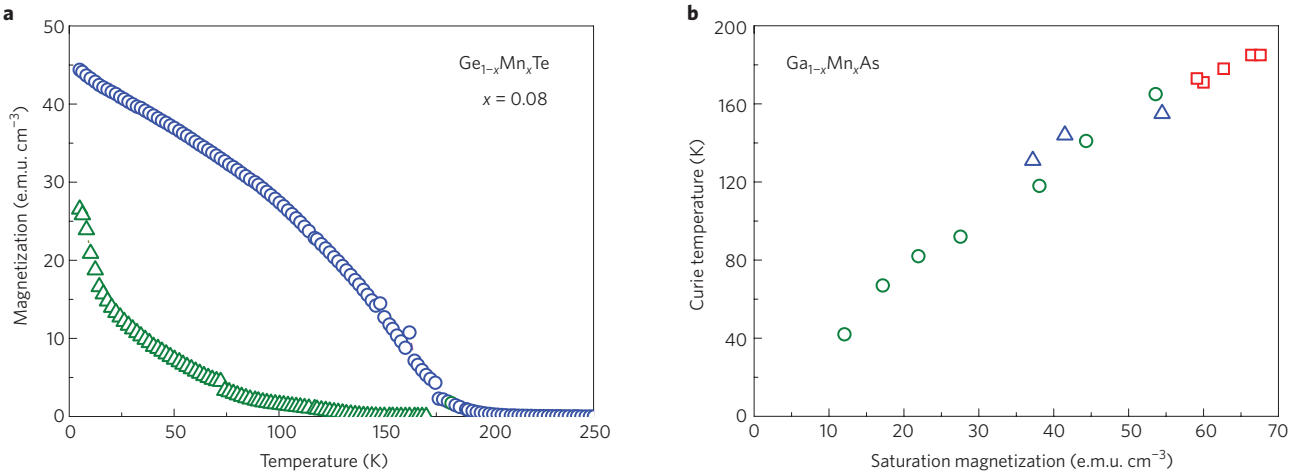


**Figure 1 | Experimental data for p-type DMS films. a**, Temperature dependence of the magnetization in (Ge,Mn)Te with high (circles) and low (triangles) hole concentrations. **b**, $T_C$ as a function of saturation magnetization for annealed (Ga,Mn)As films grown in various molecular beam epitaxy (MBE) systems. $T_C$ approaches 200 K for an effective Mn concentration of less than 10%. Figures reproduced with permission from: **a**, ref. 28, © 2008 AIP; **b**, ref. 30, © 2008 AIP.

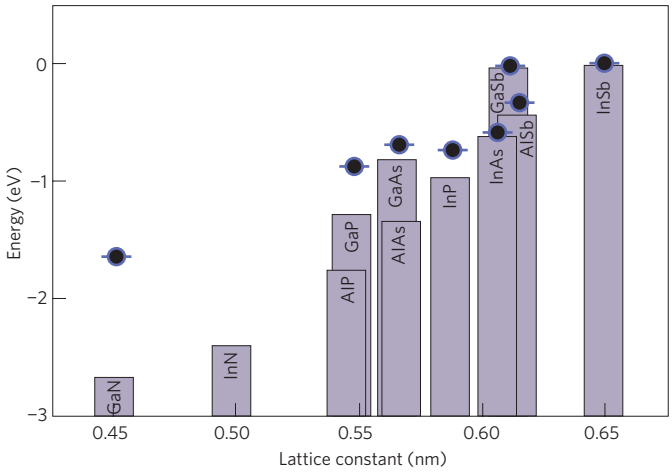


**Figure 2 | Experimental energies of Mn levels in the gaps of III–V compounds, with respect to the valence-band edges.** Bars show relative positions of valence band tops; points depict Mn acceptor levels. Reproduced with permission from ref. 56, © 2002 APS.

distributed scattering centres on the liquid of strongly correlated band carriers[51–54]. Guided by previous extensive studies of non-magnetic semiconductors, we may anticipate that rather than absolute values, only certain scaling characteristics of d.c., a.c. and tunnelling conductivity tensors can at present be interpreted theoretically near the MIT, at least at temperatures below the momentum relaxation rate. This is in contrast to thermodynamic properties, such as electronic specific heat, that are virtually unperturbed by disorder and electronic correlation at the localization boundary[52–54].

Empirically, the Anderson–Mott MIT occurs for the carrier concentration, $p_c$, at which the kinetic energy per band carrier, $E_{kin} = (3/5)E_F$ ($E_F$, Fermi energy), calculated with no disorder, decreases to about one-third of the single-impurity binding energy, $E_I$ (ref. 55). In Fig. 2, the experimental values of $E_I$ for Mn acceptors in various III–V semiconductors are shown[56]. As can be seen, $E_I$ and, thus, $p_c$ are enhanced rather drastically in comparison with non-magnetic acceptors, particularly on going from antimonides and nitrides to arsenides and phosphides. This shift is caused by the *p–d* hybridization, the importance of which increases as the cation–anion bond length decreases, ultimately resulting in a transition to the strong-coupling limit, where the hole binding is dominated by the *p–d* interaction[57].

According to the scaling theory and relevant experiments[51–54], the Anderson–Mott MIT is continuous. Hence, the carrier localization length, $\xi$, decreases gradually from infinity at the MIT to the impurity Bohr radius in the strongly localized regime, such that on a length scale shorter than $\xi$, the wavefunction retains an extended character. Such band-like carriers, whose quantum diffusivity vanishes at the MIT, were originally thought to mediate the long-range interactions between the transition-metal spins in DMSs in the whole density regime relevant to ferromagnetism[21,26].

In agreement with this view, temperature-dependent quantum corrections to the conductance[58] and the character of the tunnelling density of states[20] are consistent in (Ga,Mn)As with the expectations for Anderson–Mott localization of holes in the GaAs valence band. In particular, scanning tunnelling microscopy data[20], although presumably affected by the proximity to the surface, point directly to the crucial importance of both disorder and carrier correlation in the relevant range of Mn concentrations. At the same time, the direct visualisation[20] of spatial fluctuations in the local density of states supports the view[19] that the disappearance of ferromagnetism with carrier localization proceeds through an intermediate superparamagnetic-like phase.

In the Anderson–Mott localization model, the effects of disorder and carrier correlation appear as some broadening and Landau renormalisation of $\rho_F$, the valence-band thermodynamic density of states at $E_F$, which determines $T_C$ in the *p–d* Zener model[21,26,59]. In this context, the high-temperature thermoelectric power, $S$, is relevant, as it is a good measure of $\rho_F$ and may therefore be used to distinguish between the valence-band and impurity-band pictures. Recent measurements of $S$ in compensated (Ga,Mn)As were interpreted in terms of the anticrossing model, treating broadening of the impurity band as an adjustable parameter[49]. In this way, a small difference between the magnitudes of $S$ in (Ga,Mn)As and GaAs:Be at given hole densities was explained. I note, however, that the Mott formula, $S = (\pi^2/3e)k_B^2 T d\ln[\sigma(E_F)]/dE_F$, where $\sigma$ is the conductivity, with $\rho_F$ as for the GaAs valence band[58] describes quantitatively not only the data[49] for GaAs:Be but also that for (Ga,Mn)As, assuming that the energy dependence of the apparent hole mobility, $\mu = \sigma/ep$, where $p$ is the hole density, changes from the value expected for acoustic phonon scattering, $\mu \propto E_F^{-1/2}$, to the one specific to ionized impurity scattering, $\mu \propto E_F^{3/2}$, as the degree of compensation increases.

Furthermore, in the impurity-band models, $T_C$ is predicted to reach a maximum when the Fermi level is shifted across the peak in the density of impurity states. The accumulated data for (Ga,Mn)As show that the value of $T_C$ decreases monotonically when the hole concentration is decreased by gating[60] or by increasing the concentration of compensating donors[49,61,62]. However, it was found in recent studies that $T_C$ is actually increased by co-doping with Si donors[48] and, moreover, goes through a maximum as a result of modulation doping by Be acceptors[63]. As underlined in these works, the findings are consistent with the impurity-band scenario. But the presented data reveal that the increase in $T_C$ in Si-doped samples

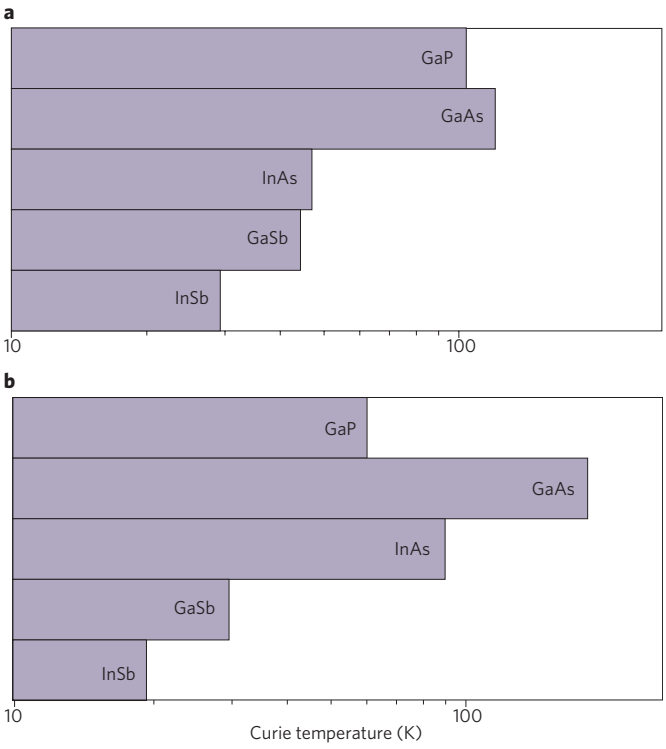


**Figure 3 | Predictions of the *p–d* Zener model compared with experimental data for p-type (III,Mn)V DMSs. a**, computed values of $T_C$ for various p-type semiconductors containing 5% Mn and $3.5 \times 10^{20}$ holes cm$^{-3}$ (the value for (In,Mn)Sb is taken from ref. 69). Reproduced with permission from ref. 21, © 2000 AAAS. **b**, Highest reported values for (Ga,Mn)P (ref. 65), (Ga,Mn)As (refs 29, 30), (In,Mn)As (ref. 66), (Ga,Mn)Sb (ref. 67) and (In,Mn)Sb (ref. 68).

and its decrease in the Be case are respectively associated with an enlargement or a reduction of the saturation value of magnetization and, thus, of the Mn concentration, $x_{eff}$, that determines $T_C$. The results[48,63] can therefore be explained by the known anticorrelation[64] between $x_{eff}$ and the density of holes during the epitaxy, which here is reduced by Si donors[48] or 'siphoned off' from the Be-doped barrier into the grown quantum well[63].

At the same time, low values of $\mu$ (less than 10 $cm^2\ V^{-1}s^{-1}$), taken as evidence for a large effective hole mass[35,36], can be explained by the proximity to the MIT, where charge diffusion is much reduced by quantum localization effects. Furthermore, referring to a shift of an a.c. conductivity maximum with the hole density[35], which contradicts the expectations of the Drude–Boltzmann theory, I emphasize that the frequency-dependent conductance near the MIT is dominated, at least up to frequencies of the order of the momentum relaxation rate, by quantum localization effects[52–54], whose presence may account for the observed anomalies.

## $T_C$ for carrier-mediated ferromagnetism in III–V DMSs

In Fig. 3, the highest values of $T_C$ found so far in p-type Mn-based III–V DMSs[29–31,65–68] are shown and compared with the early predictions of the *p–d* Zener model[21,69] for fixed values of the Mn and hole concentrations. We see that the theory reproduces the chemical trends and describes semi-quantitatively the absolute values of $T_C$. The observed trend reflects a decrease in the *p–d* exchange energy for larger cation–anion distances as well as an enhanced role of the competing spin–orbit interaction in materials with heavier anions. At the same time, the dependence of $T_C$ on the effective Mn concentration[30,61] and the density of itinerant holes, changed in (Ga,Mn)As by Mn concentration, donor compensation or by gating[60,61,70], is consistent with the *p–d* Zener model. Furthermore, the model properly describes the magnitude of the strain-induced magnetic anisotropy[71].

Unfortunately, a more detailed comparison between theory and experiment is hampered by the lack of information on short-range antiferromagnetic interactions, which become progressively more important as the Mn concentration increases, and by enduring difficulties in the accurate determination of the Mn and hole densities.

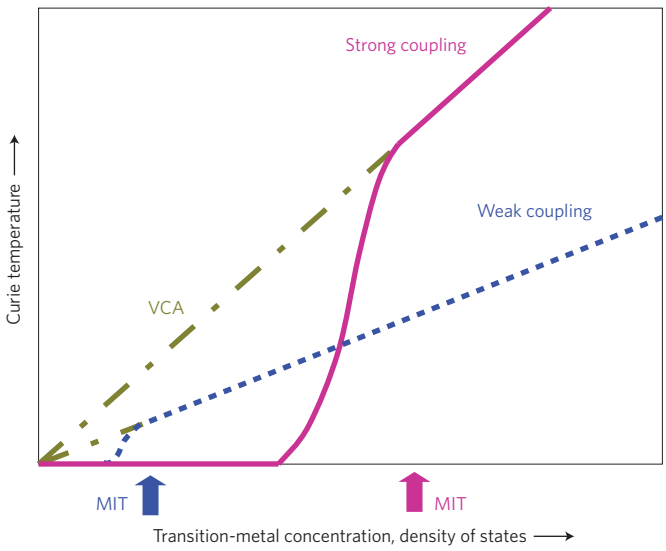


**Figure 4 | Dependence of $T_C$ on the concentration of magnetic impurities and density of hole states at the Fermi level for weak and strong coupling.** Higher values of $T_C$ are predicted within the virtual-crystal approximation (VCA) and the molecular-field approximation for strong coupling. However, the region where the holes are localized and do not mediate the spin–spin interaction is wider in the strong-coupling case. Reproduced with permission from ref. 57, © 2008 APS.

According to three-dimensional atom probe investigations[72], Mn ions are distributed randomly in (Ga,Mn)As at a resolution of 1 nm. Nevertheless, from previous channelling studies[73] we know that because of self-compensation, a considerable portion of Mn ions occupy interstitial positions and, hence, act as double donors[70], compensating partly holes as well as Mn spins, owing to a supposedly antiferromagnetic coupling between interstitial and substitutional Mn pairs. Furthermore, a large fraction of Mn ions, particularly in annealed samples, reside in a MnO layer near the surface.

The applicability of the *p–d* Zener model to (Ga,Mn)As and related systems has been confirmed by *ab initio* studies in which inaccuracies of the local spin density approximation (LSDA) are partly compensated by the LSDA + *U* approach[74] or by self-interaction corrections[75]. Furthermore, a number of ferromagnetism models, tailored to DMSs without holes in the valence band, have been put forward, as reviewed elsewhere[40,70]. It is still unclear, however, whether long-range ferromagnetic order can settle above 10 K, for example, if holes are bound to individual Mn acceptors in DMSs (the strongly localized regime), such that the exchange interaction decays exponentially with the distance between spin pairs. So far, a ferromagnetic coupling between isolated nearest-neighbour Mn pairs has been revealed by scanning tunnelling microscopy in GaAs:Mn and analysed successfully in terms of a tight-binding model[76].

It is instructive to compare (Ga,Mn)As, (Ga,Mn)P and (Ga,Mn)N containing the same concentration of Mn, for example 6%, as among these three material systems $E_I$ differs significantly, according to the data collected in Fig. 2. The (Ga,Mn)As films containing 6% Mn and typically more than $10^{20}$ holes $cm^{-3}$ are on the metallic side of the MIT[22]. In the case of $Ga_{0.94}Mn_{0.06}P$, $E_I$ is large enough to result in hole localization. However, the conductance activation energy[65], which is a factor of ten smaller than $E_I$ for GaP:Mn, indicates that the holes are only weakly localized. Accordingly, the *p–d* Zener model can serve to explain the origin of ferromagnetic correlations in this case also.

In contrast, no information on hole transport is available for the MBE-grown $Ga_{0.94}Mn_{0.06}N$ film[77], indicating that the strongly localized regime is reached. In line with the notion that itinerant holes are necessary to observe a coupling between diluted spins, the observed $T_C$ is as low as 8 K. In the schematic diagram in Fig. 4, (Ga,Mn)N represents a strong-coupling case, where the holes remain localized over a wide rage of Mn concentrations, in contrast to both $Ga_{1-x}Mn_xAs$, for which the MIT appears below $x = 2\%$ for weakly compensated samples[50], and (Ga,Mn)P, which is an intermediate case.

It is worth noting that there are indications of a non-random Mn distribution in another (Ga,Mn)N film grown by MBE (ref. 78). This may suggest that $T_C = 8$ K actually constitutes an upper limit for $T_C$ in $Ga_{0.94}Mn_{0.06}N$. These findings demonstrate, therefore, that the current *ab initio* theory[40], which predicts that $T_C \gtrsim 60$ K for $Ga_{0.94}Mn_{0.06}N$, still overestimates the significance of ferromagnetic couplings in the case of DMSs with no valence-band holes.

## Competing interactions in p-type II–VI DMSs

In II–VI compounds, where Mn is an isoelectronic impurity, it is possible to control the spin and the carrier density independently. However, at given Mn and hole concentrations, $T_C$ is much lower in II–VI DMSs than in III–V compounds, owing to a destructive influence of the short-range antiferromagnetic superexchange. This effect is less relevant in III–V DMSs, where $Mn^{2+}$ centres are negatively charged, such that the enhanced hole density at closely lying Mn pairs compensates, at least partly, short-range antiferromagnetic interactions[21].

Following its theoretical prediction[26], carrier-induced ferromagnetism was revealed in modulation-doped p-type (Cd,Mn)Te/(Cd,Zn,Mn)Te:Mg heterostructures using photoluminescence spectroscopy[5,59]. The character of the magnetic anisotropy, as well as

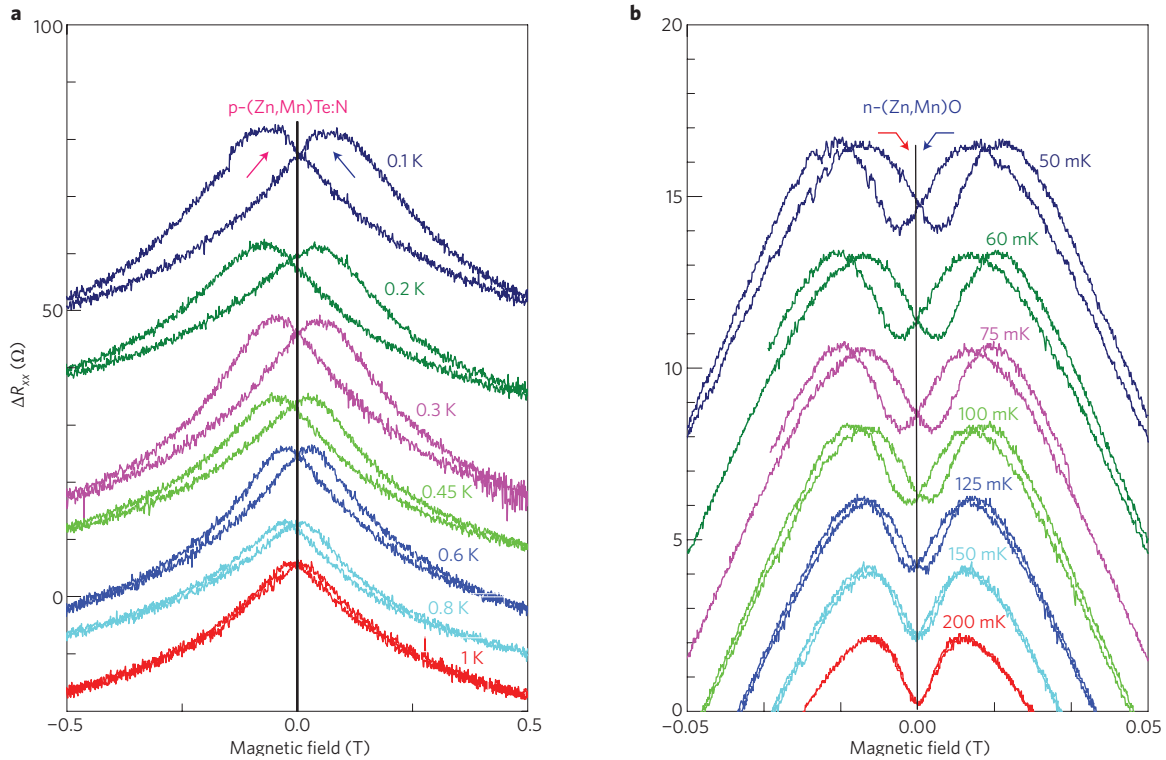


**Figure 5 | Resistive indications of ferromagnetism in p-$Zn_{0.981}Mn_{0.019}$Te:N and n-$Zn_{0.97}Mn_{0.03}$O:Al. a**, The temperature dependence of the hysteresis widths at low temperatures and the magnetic susceptibility measurements above 2 K indicate that $T_C$ = 1.45 ± 0.05 K in p-$Zn_{0.981}Mn_{0.019}$Te:N with a hole concentration of 1.2 × $10^{20}$ $cm^{-3}$. **b**, The temperature and field scales are an order of magnitude smaller in n-$Zn_{0.97}Mn_{0.03}$O:Al with an electron concentration of 1.4 × $10^{20}$ $cm^{-3}$, where $T_C$ = 160 ± 20 mK. Solid lines show changes of longitudinal resistivity in the magnetic field, $\Delta R_{xx}$, as measured for decreasing (blue arrows) and increasing (red arrows) the field. Curves obtained at different temperatures are vertically shifted for clarity. The width of the hysteresis loops is seen to increase on lowering the temperature. Figures reproduced with permission from: **a**, ref. 80, © 2001 APS; **b**, ref. 81, © 2001 Springer.

the magnitude of $T_C$ and its evolution with the hole density, which are controlled by the electric field and the illumination, was found to be consistent with the *p–d* Zener model adapted for this low-dimensionality system. Interestingly, however, no magnetic hystereses have been detected below $T_C$. According to extensive Monte Carlo simulations, the effect reflects fast magnetization dynamics generated by the antiferromagnetic interactions at the borders of the hole layer[79].

Ferromagnetic signatures were also found in epilayers of p-type (Zn,Mn)Te:N (refs 6, 80) and n-type (Zn,Mn)O:Al (ref. 81). As shown in Fig. 5, for a high carrier density the low-temperature resistance becomes hysteretic. This points to the appearance of ferromagnetic order and directly demonstrates the existence of a strong coupling between carriers and Mn spins. The temperature dependence of the coercive force, together with magnetic susceptibility measurements above 2 K, point to a magnetic ordering temperature of $T_C$ = 1.45 K in the case of $Zn_{0.0981}Mn_{0.019}$Te:N with 1.2 × $10^{20}$ holes $cm^{-3}$. This value is in agreement with the predictions of the *p–d* Zener model, provided that the aforementioned antiferromagnetic interactions and the spin–orbit interaction are taken carefully into account[80]. A similar experimental procedure shows that $T_C$ = 160 mK in the case of $Zn_{0.097}Mn_{0.03}$O:Al with 1.4 × $10^{20}$ electrons $cm^{-3}$ (ref. 81). Given the difference between relevant parameters and, in particular, the three-fold-greater amplitude of the exchange integral in the *p–d* case than in the *s–d* case, the experimentally observed difference in the $T_C$ values between p-type and n-type materials can be readily explained.

## Carrier-mediated ferromagnetism with higher $T_C$

A number of authors have reported the observation of room-temperature ferromagnetism in various semiconductors and oxides containing supposedly randomly distributed localized spins. However, it is probably fair to say that so far none of these findings has been confirmed by other groups and none has resulted in the demonstration of a device structure working at room temperature. As I will argue in the following sections, if this robust ferromagnetism is not an experimental artefact it can be explained by assuming a non-random distribution of the magnetic ions.

It seems that despite ten years of extensive investigations, the conditions under which room-temperature ferromagnetism was predicted for nitrides and oxides[21] have not yet been experimentally met. In particular, no (Ga,Mn)N, (Zn,Mn)O or related compound containing a few per cent of randomly distributed magnetic cations and a few $10^{20}$ delocalized or weakly localized holes per cubic centimetre has so far been synthesized. However, in annealed (Ga,Mn)As the effective Mn concentration, as judged from the saturation magnetization, now approaches 10%, although $T_C$ remains below 200 K.

Can, therefore, carrier-mediated, indirect spin–spin coupling produce ferromagnetic ordering that is stable up to room temperature? I note that a variant of the *p–d* Zener model explains the origin of ferromagnetism in double-perovskite compounds, such as $Sr_2CrReO_6$, where $T_C$ can reach 625 K (ref. 82) despite the distance between localized spins being as large as 0.6–0.7 nm. This shows the potential of this mechanism to support high-temperature ferromagnetism possibly also in DMSs, where, in GaN and ZnO, the distance between second-nearest-neighbour cations is less than 0.5 nm.

However, the obvious difficulty is to synthesize a p-type, wide-bandgap DMS system in which the hole density is large enough to result in a MIT even in the strong-coupling case, as sketched in Fig. 4. It has been suggested[57]—but not yet verified experimentally—that once the MIT is reached, and the bound states therefore washed out by many-body screening, high values of $T_C$ (expected in the virtual-crystal and molecular-field approximations[21]) should emerge. Various methods allowing us to enlarge the hole density

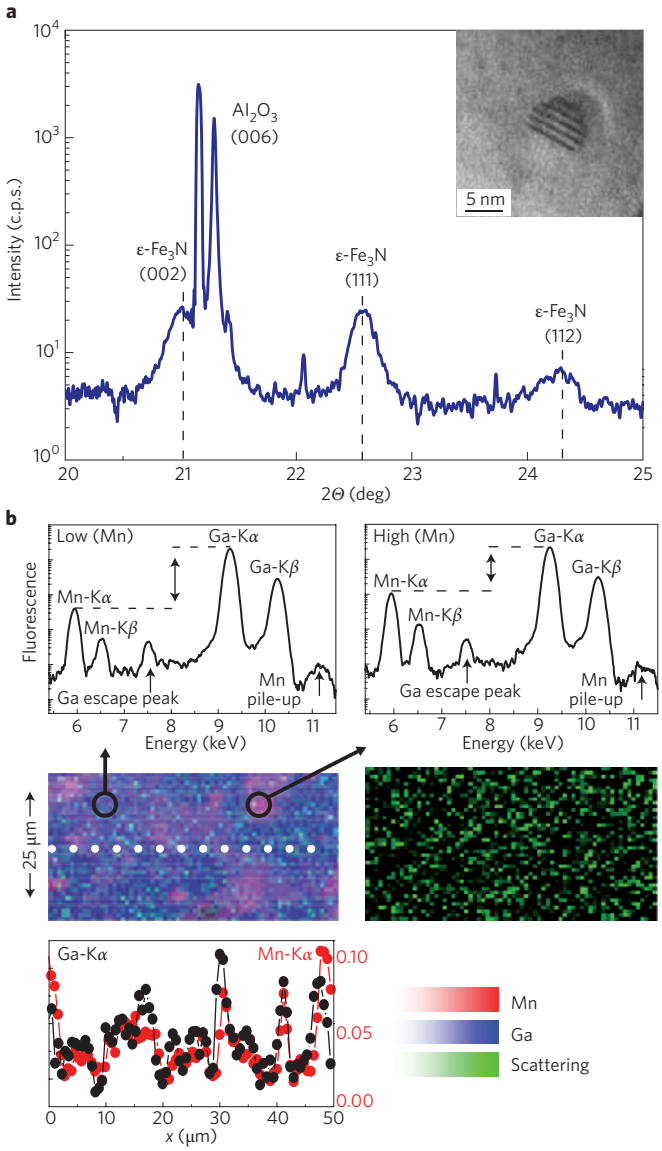


**Figure 6 | Evidence for crystallographic and chemical phase separations in DMSs. a**, Synchrotron X-ray diffraction (main panel) and transmission electron microscopy (inset) results for (Ga,Fe)N, showing the precipitation of hexagonal ε-$Fe_3N$ nanocrystals. c.p.s., counts per second; $\Theta$, diffraction angle. Modified from ref. 89, © 2008 APS. **b**, Element-specific synchrotron radiation microprobe analysis of (Ga,Mn)N showing aggregation of Mn cations. X-ray fluorescence spectra are shown for Mn-poor and Mn-rich regions (low (Mn) and high (Mn), respectively). Red, blue and green in the middle panels correspond to the spatially resolved Mn-K$\alpha$, Ga-K$\alpha$ fluorescence line and inelastic (Compton) scattering signal, respectively. Ga (black) and Mn (red) profiles along the white scan line are shown in the lowest panel, indicating the formation of regions rich in Mn and Ga. Reproduced with permission from ref. 78, © 2005 AIP.

above $10^{20}$ $cm^{-3}$ without increasing the degree of disorder, such as gating and doping in a modulated fashion, or exploiting interfacial electric fields, may lead to semiconductors with high, tunable $T_C$ values. I note that continued progress in gate oxide deposition[11,19] allows interfacial charge densities of the order of $3 \times 10^{13}$ $cm^{-2}$, that is, up to about $3 \times 10^{20}$ $cm^{-3}$.

## Origin of observed high-temperature ferromagnetism

Perhaps the most surprising development of the past decade in the science of magnetic materials is the abundant observations of spontaneous magnetization persisting to above room temperature in semiconductors and oxides, in which no ferromagnetism was expected at any temperature, particularly in the *p–d* Zener model. These findings offer the prospect of a range of spintronic functionalities much wider than could initially be anticipated. At the same time, they have generated a considerable theoretical effort resulting in the proposal of several novel mechanisms of exchange interaction between diluted spins, designed to interpret robust ferromagnetism in magnetically doped or even magnetically undoped systems. Nevertheless, there seems to be no visible convergence between particular experimental findings and theoretical models.

Over the past years, we have started to realize that open *d* shells of magnetic impurities in non-magnetic solids not only provide localized spins but also, through hybridization with band states, contribute significantly to the cohesive energy, particularly if transition-metal impurities occupy neighbouring sites. The resulting attractive force between magnetic cations leads to their aggregation, invalidating the main premise of DMS and DMO physics, namely that concerning the random distribution of transition-metal spins. It may be anticipated that the magnetic nanocrystals formed in this way take the crystallographic form imposed by the matrix. Accordingly, the properties of these condensed magnetic semiconductors (CMSs) may yet be not included in materials compendia, and it is a-priori unknown whether they are metallic or insulating, or whether they have ferromagnetic, ferrimagnetic or antiferromagnetic spin order. However, because CMS nanocrystals contain a high concentration of the magnetic constituent, their spin ordering temperature is expected to be relatively high, typically above room temperature.

The experimental detection of a non-random spin distribution and possible contamination has been highly challenging in DMS research[39]. Only recently has the actual spatial distribution of transition-metal cations in some DMSs been established, by application of state-of-the-art, element-specific nano-characterization tools. Although some cases concern elemental ferromagnetic metal nanoparticles, for instance Co in ZnO (refs 83, 84), usually transition-metal compounds are involved. Taking (Ga,Fe)N as an example, I note that according to standard laboratory high-resolution X-ray diffraction, the incorporation of Fe simply leads to a broadening of the GaN-related diffraction maxima without revealing any secondary phases[85]. In contrast, the use of a much brighter synchrotron source has allowed the detection of precipitates in the same samples, as shown in Fig. 6, a counterpart of MnAs nanocrystals in GaAs (refs 86, 87). The appearance of crystallographic phase separation in (Ga,Fe)N is supported by studies[88] of near-edge X-ray absorption fine structure. The dominant ferromagnetic precipitate was identified as $Fe_3N$, but in some cases nanocrystals in the form of an elemental ferromagnetic metal, Fe in this case, are also visible[89]. At the same time, transmission electron microscopy with appropriate mass and strain contrast, and electron dispersive spectroscopy, not only corroborated the outcome of synchrotron X-ray diffraction but also revealed the aggregation of magnetic cations without distorting the host wurtzite structure under certain growth conditions[89]. This chemical phase separation is known in the DMS literature as spinodal decomposition, independently of the microscopic mechanism leading to the aggregation of the transition-metal cations. I note that although X-ray magnetic circular dichroism and related techniques constitute a powerful element-specific tool for revealing relationships between ferromagnetism and crystallographic phase separation[84], they cannot in general tell whether the ferromagnetism originates from diluted spins or results from a chemical phase separation.

The application of transmission electron microscopy with electron dispersive spectroscopy made it possible to find evidence for the chemical phase separation in annealed (Ga,Mn)As (refs 87, 90), (Zn,Cr)Te (ref. 91), (Al,Cr)N and (Ga,Cr)N (ref. 92),

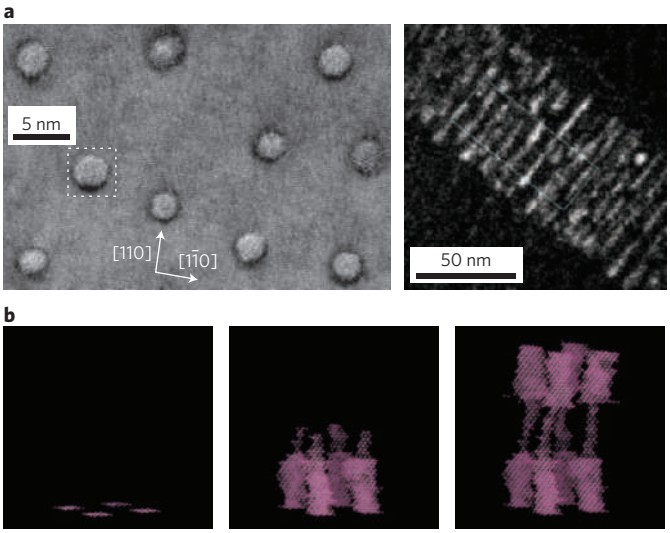


**Figure 7 | Formation of nanocolumns DMSs by aggregation of transition-metal cations. a**, Mn-rich nanocolumns in (Ge,Mn) shown by high-resolution transmission electron microscopy (left, plan view showing nanocolumns as dots on the surface) and Mn chemical maps (right, bright regions show Mn atoms substituting Ge in the invisible Ge lattice). **b**, Monte Carlo simulation of chemical phase separation in (Zn,Cr)Te with seeding to initiate the growth of nanocolumns and control of their diameter by Cr flux; pink points show positions of Cr atoms substituting Zn in the invisible ZnTe lattice. Figures reproduced with permission from: **a**, ref. 93, © 2006 NPG; **b**, ref. 95, © 2007 Wiley.

whereas according to the results summarized in Fig. 6, hexagonal nanocrystals were detected in (Ga,Mn)N. Finally, I mention the case of (Ge,Mn), where under suitable growth conditions quasi-periodically arranged nanocolumns are observed[93], as shown in Fig. 7. A tendency to form nanocolumns was also reported for (Al,Cr)N (ref. 92) and (Zn,Cr)Te (ref. 94). This demonstrates that growth conditions can assist in controlling the nanocrystal shape. Interestingly, these two kinds of nanocrystal form were reproduced by Monte Carlo simulations[95]. Furthermore, a strict correlation between ferromagnetic features and the presence of CMS nanocrystals has been demonstrated for these systems. However, the identification of the dominant microscopic mechanisms leading to robust spin ordering, that is, to a large $T_C$ and magnetic anisotropy, awaits detailed experimental and theoretical studies of particular combinations of CMSs and hosts.

As expected, the lowering of the growth temperature and/or the increase of the growth rate[89] hampers the aggregation of magnetic cations. Moreover, it has been suggested that it is possible to change the transition-metal charge state and, therefore, the aggregation energy by co-doping with shallow donors or acceptors[96,97]. This way of affecting the transition-metal valency stems from the presence of bandgap states derived from the *d* orbitals. These states trap carriers supplied by shallow impurities, altering the charge state of the magnetic cations and hence modifying their mutual interactions. Accordingly, co-doping of DMSs and DMOs with shallow acceptors or donors, during either growth or post-growth processing, modifies the valence, providing a powerful means of controlling the aggregation of magnetic cations. These predictions are corroborated by experimental finding for (Ga,Mn)N (ref. 39), (Zn,Cr)Te (ref. 91) and (Ga,Fe)N (ref. 89), where remarkable changes in the ferromagnetic characteristics on co-doping with shallow impurities have been found and correlated with the transition-metal distribution.

Finally, I note that, depending on the growth conditions, CMS nanocrystals can be distributed randomly or can accumulate either at the interface with the buffer or at the film surface. Furthermore, transition-metal impurities may decorate or diffuse along extended defects such as dislocations or grain boundaries[98]. This seems to explain an inverse correlation, noted by some authors in the case of oxides[84,99], between sample quality and the appearance of high-$T_C$ ferromagnetism.

## Some modelling

The above qualitative considerations are supported by *ab initio* studies. For instance, the computed energy change associated with bringing two Ga-substitutional Mn atoms to the nearest-neighbour cation position is $E_d = -120$ meV in GaAs and −300 meV in GaN, and reaches −140 and −350 meV in the cases of a cation-substitutional Cr nearest-neighbour pair in ZnTe and GaN, respectively[91,100]. In contrast, there is virtually no energy change associated with bringing two Zn-substitutional Mn atoms to the nearest-neighbour cation sites in (Zn,Mn)Te, where $E_d = 21$ meV (ref. 91). This can be associated with the fact that the Mn *d* states little perturb the $sp^3$ tetrahedral bonds as both the lower $d^5$ (donor) and the upper $d^6$ (acceptor) Hubbard levels are respectively well below and above the band edges in II–VI compounds[101], meaning that there is no appreciable difference between the band hybridization involving Zn and that involving Mn. This conclusion is consistent with the high solubility of Mn in II–VI compounds and the apparently random distribution of Mn in these systems[102].

To model the effect of co-doping, I note that the energy of the screened Coulomb interaction between two elementary charges residing on the nearest-neighbour cation sites in the GaAs lattice is $E_d = -280$ meV. This value indicates that a change in the charge state can affect the aggregation significantly, as the gain of energy associated with bringing two Mn atoms close together is, recall[100], $E_d = -120$ meV. Accordingly, a surplus of charge on transition-metal ions, relative to non-magnetic cations, caused by co-doping with shallow dopants can counteract the gain of energy stemming from *p–d* hybridization and impede the nanocrystal assembly[96,97]. This picture is confirmed by *ab initio* computations within the LSDA for $(Ti,Cr)O_2$ (ref. 96) and (Zn,Cr)Te (refs 91, 103). As shown in Fig. 8, $E_d$ attains a minimum in ZnTe when the two Cr cations are in the 2+ charge state[103] ($d^4$ configuration). However, the computational results shown in the same plot indicate that $E_d$ goes through a minimum in the $Cr^{2+}$ case also in GaAs, rather than in the case of $Cr^{3+}$ pairs, as might be expected for III–V compounds.

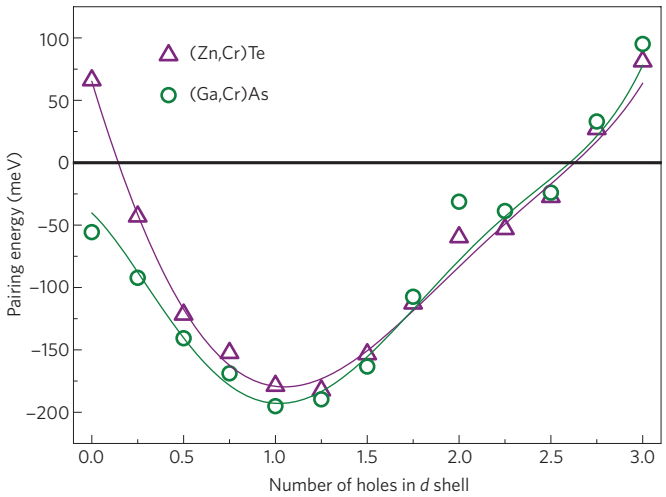


**Figure 8 | Computed energy change $E_d$ in ZnTe and GaAs**. Energy change (pairing energy) resulting from bringing two Cr impurities to the nearest-neighbour cation positions, as a function of the number of holes in the Cr $d^5$ shell. Reproduced with permission from ref. 103, © 2008 IOP.

## From dilute to nanocomposite systems

In view of the above discussion, the incorporation of transition-metal impurities into semiconductors not only bridges ferromagnetic and semiconductor capabilities but also offers a way to develop a new kind of nanocomposite system consisting of ferromagnetic and metallic nanocrystals coherently buried in a semiconductor host. It is believed that the application of embedded metallic and semiconducting nanocrystals will revolutionize the performance of various commercial devices, such as flash memories, low-current semiconductor lasers and single-photon emitters. The use of nanocomposite semiconductor–ferromagnet systems could be similarly far reaching, owing to their unique capabilities and to the possibility of controlling the shape (nanodots versus nanocolumns) and size with growth parameters and co-doping during the epitaxial process.

It has already been demonstrated that these nanocomposites show strong magnetotransport and magneto-optical effects[90,91] that could possibly allow them to be used as magnetic field sensors as well as in magneto-optical devices. In particular, a combination of a strong magnetic circular dichroism specific to ferromagnetic metals and weak losses characterizing the semiconductor hosts suggests possible functionalities as optical isolators as well as three-dimensional, tunable photonic crystals and spatial light modulators for advanced photonic applications. As an interesting recent development, a spin battery effect has been demonstrated in the GaAs:MnAs system in a magnetic field[104].

As shown in Fig. 7, the controlled growth of nanocolumns of a ferromagnetic metal, for example a dense array of magnetic tunnel junctions[95] or Coulomb blockade devices, can allow fabrication *in situ*. Thus, the media in question can be used for low-power, high-density magnetic storage, including spin-torque magnetic random access memories and three-dimensional, domain-wall-based racetrack memories. Sufficiently high tunnelling magnetoresistance could be used to realize field-programmable logic (tunnelling-magnetoresistance-based connecting/disconnecting switches) and even all-magnetic logic, characterized by low power consumption and radiation hardness. Furthermore, embedded metallic nanostructures may serve as building blocks for all-metallic nanoelectronics and for high-quality nanocontacts in nanoelectronics, optoelectronics and plasmonics, and may constitute media for thermoelectric applications[105]. It is also worth mentioning the importance of hybrid semiconductor–ferromagnet systems in various proposals for scalable quantum processors.

## $d^0$ ferromagnetism and beyond

Organic ferromagnets and quantum Hall ferromagnets are proof that ferromagnetism is possible in materials without magnetic ions, although the corresponding $T_C$ values are so far low, typically less than 20 K. It has been suggested that robust ferromagnetism can also appear in certain zincblende metals such as CaAs, and be driven by a Stoner instability in the narrow heavy-hole band[106,107], a prediction awaiting experimental confirmation.

It has been known for a long time that a number of defects or non-magnetic impurities form localized paramagnetic centres in various hosts. Some of these states might show a large intracentre correlation energy, $U$, that could ensure adequate stability of the spins even if their density increases or the material is co-doped with shallow impurities. It is therefore tempting to relate the presence of unexpected high-temperature ferromagnetism in various oxides and carbon derivates to magnetic moments residing on non-magnetic defects or impurities rather than on open $d$ shells of transition metals[38,108].

As shown theoretically[109], a sizable exchange interaction takes place between valence-band holes residing on non-magnetic acceptors and electrons in the conduction band. This demonstrates that band carriers can mediate a Zener-type coupling between spins localized on defect centres. Furthermore, if the spin concentration increases, such that either the Hubbard–Mott or the Anderson–Mott transition is reached, the double-exchange or Stoner-like mechanism might appear[46]. However, in each of these cases a clear correlation between magnetic and transport properties should be visible, analogous to that observed routinely in manganites, (Ga,Mn)As and p-(Zn,Mn)Te. In particular, the fabrication of a spintronic structure—such as a magnetic tunnel junction—that works at high temperatures, would be a strong confirmation of the existence of spin transport in these challenging systems. Alternatively, defects and impurities, similarly to transition-metal dopants, could form high-spin aggregates in certain hosts. In this case, the presence of ferromagnetic-like features should correlate with the existence of defect agglomerations that can be revealed using state-of-the-art nano-characterization tools.

So far, suggestions concerning defect-related, high-temperature ferromagnetism come only from global magnetization measurements. Therefore, it seems more natural to assume at this stage that a small number of magnetic nanoparticles—which escaped detection—account for the high-temperature ferromagnetic-like behaviour of nominally non-magnetic insulators and semiconductors. Such nanoparticles could be introduced during synthesis or post-growth processing, and can reside in the sample volume not only at dislocations and grain boundaries but also on the surface, on the interface and in the substrate. An instructive example is provided by the case of porous silicon[110].

## Outlook

Where do we then head after these ten years? There is no doubt that (Ga,Mn)As and related compounds have considerably strengthened their position as outstanding systems in which to develop and test novel functionalities unique to the combination of ferromagnetic and semiconductor properties. Many of the associated concepts[8], such as spin injection, electric field control of $T_C$ and magnetization direction, tunnelling anisotropic magnetoresistance in planar junctions and in the Coulomb blockade regime, and current-induced domain displacement without the assistance of a magnetic field, are now being developed in devices involving ferromagnetic metals, which may function at ambient temperatures.

However, a further increase in $T_C$, over the current record value of 190 K, continues to be a major goal in the field of DMSs. This may be achieved by progress in materials, defects and interfaces engineering, leading to higher spin and hole densities, and by exploiting proximity effects at ferromagnet–semiconductor junctions[111].

As emphasized in this Review, investigations of magnetically doped semiconductors and oxides have presented us with unexpectedly challenging issues intractable by conventional materials characterization, computational and theoretical tools. In addition to the interplay among phenomena specific to strongly correlated and disordered systems, encountered in doped semiconductors and manganites, DMSs and DMOs introduce a fundamentally new ingredient that results from an unanticipated correlation in the magnetic ion distribution. We are now learning how to visualize and control the magnetic ion aggregation to develop methods of producing lateral and vertical distributions, as well as different shapes, of magnetic nanocrystals on demand. The ferromagnetic metal/semiconductor nanocomposites fabricated in this way offer a spectrum of so far unexplored possibilities in various fields of materials science and device physics.

Are there only two classes of magnetically doped semiconductor and oxide with ferromagnetic features above, for instance, 10 K? Are ferromagnetic correlations mediated by valence-band holes and embedded magnetic nanocrystals the only sources of spontaneous magnetization in these systems? We will see in the years to come whether the widely discussed ferromagnetic double exchange and superexchange can lead to robust spin ordering in dilute systems. We

may also learn how to exploit strong antiferromagnetic interactions inherent in magnetic insulators to develop ferrimagnetic or antiferromagnetic[112] functional nanostructures, in which partly or entirely reduced stray fields and, hence, magnetic cross-talk will be an asset.

## References


1. Story, T., Galazka, R. R., Frankel, R. B. & Wolff, P. A. Carrier-concentration-induced ferromagnetism in PbSnMnTe. *Phys. Rev. Lett.* **56,** 777–779 (1986).
2. Ohno, H., Munekata, H., Penney, T., von Molnàr, S. & Chang, L. L. Magnetotransport properties of p-type (In, Mn)As diluted magnetic III-V semiconductors. *Phys. Rev. Lett.* **68,** 2664–2667 (1992).
3. Ohno, H. *et al.* (Ga, Mn)As: a new diluted magnetic semiconductor based on GaAs. *Appl. Phys. Lett.* **69,** 363–365 (1996).
4. Van Esch, A. *et al.* Interplay between the magnetic and transport properties in the III-V diluted magnetic semiconductor $Ga_{1-x}Mn_xAs$. *Phys. Rev. B* **56,** 13103–13112 (1997).
5. Haury, A. *et al.* Observation of a ferromagnetic transition induced by two-dimensional hole gas in modulation-doped CdMnTe quantum wells. *Phys. Rev. Lett.* **79,** 511–514 (1997).
6. Ferrand, D. *et al.* Carrier-induced ferromagnetic interactions in p-doped $Zn_{1-x}Mn_xTe$ epilayers. *J. Cryst. Growth* **214–215,** 387–390 (2000).
7. Awschalom, D. D. & Flatté, M. E. Challenges for semiconductor spintronics. *Nature Phys.* **3,** 153–159 (2007).
8. Dietl, T., Awschalom, D. D., Kaminska, M. & Ohno, H. (eds) *Spintronics* (Semiconductors and Semimetals 82, Elsevier, 2008).
9. Ohno, Y. *et al.* Electrical spin injection in a ferromagnetic semiconductor heterostructure. *Nature* **402,** 790–792 (1999).
10. Ohno, H. *et al.* Electric-field control of ferromagnetism. *Nature* **408,** 944–946 (2000).
11. Chiba, D. *et al.* Magnetization vector manipulation by electric fields. *Nature* **455,** 515–518 (2008).
12. Chernyshov, A. *et al.* Evidence for reversible control of magnetization in a ferromagnetic material by means of spin–orbit magnetic field. *Nature Phys.* **5,** 656–659 (2009).
13. Gould, C. *et al.* Tunnelling anisotropic magnetoresistance: a spin-valve like tunnel magnetoresistance using a single magnetic layer. *Phys. Rev. Lett.* **93,** 117203 (2004).
14. Wunderlich, J. *et al.* Coulomb blockade anisotropic magnetoresistance effect in a (Ga, Mn)As single-electron transistor. *Phys. Rev. Lett.* **97,** 077201 (2006).
15. Yamanouchi, M., Chiba, D., Matsukura, F. & Ohno, H. Current-induced domain-wall switching in a ferromagnetic semiconductor structure. *Nature* **428,** 539–541 (2004).
16. Matsumoto, Y. *et al.* Room temperature ferromagnetism in transparent transition metal-doped titanium dioxide. *Science* **291,** 854–856 (2001).
17. Bonanni, A. & Dietl, T. A story of high-temperature ferromagnetism in semiconductors. *Chem. Soc. Rev.* **39,** 528–539 (2010).
18. Sheu, B. L. *et al.* Onset of ferromagnetism in low-doped $Ga_{1-x}Mn_xAs$. *Phys. Rev. Lett.* **99,** 227205 (2007).
19. Sawicki, M. *et al.* Experimental probing of the interplay between ferromagnetism and localization in (Ga,Mn)As. *Nature Phys.* **6,** 22–25 (2010).
20. Richardella, A. *et al.* Visualizing critical correlations near the metal-insulator transition in $Ga_{1-x}Mn_xAs$. *Science* **327,** 665–669 (2010).
21. Dietl, T., Ohno, H., Matsukura, F., Cibert, J. & Ferrand, D. Zener model description of ferromagnetism in zinc-blende magnetic semiconductors. *Science* **287,** 1019–1022 (2000).
22. Matsukura, F., Ohno, H., Shen, A. & Sugawara, Y. Transport properties and origin of ferromagnetism in (Ga,Mn)As. *Phys. Rev. B* **57,** R2037–R2040 (1998).
23. Okabayashi, J. *et al.* Core-level photoemission study of $Ga_{1-x}Mn_xAs$. *Phys. Rev. B* **58,** R4211–R4214 (1998).
24. Linnarsson, M., Janzén, E., Monemar, B., Kleverman, M. & Thilderkvist, A. Electronic structure of the GaAs:MnGa center. *Phys. Rev. B* **55,** 6938–6944 (1997).
25. Zener, C. Interaction between the *d* shells in the transition metals. *Phys. Rev.* **81,** 440–444 (1951).
26. Dietl, T., Haury, A. & d'Aubigne, Y. M. Free carrier-induced ferromagnetism in structures of diluted magnetic semiconductors. *Phys. Rev. B* **55,** R3347–R3350 (1997).
27. Jungwirth, T., Atkinson, W. A., Lee, B. & MacDonald, A. H. Interlayer coupling in ferromagnetic semiconductor superlattices. *Phys. Rev. B* **59,** 9818–9821 (1999).
28. Fukuma, Y. *et al.* Carrier-induced ferromagnetism in $Ge_{0.92}Mn_{0.08}Te$ epilayers with a Curie temperature up to 190 K. *Appl. Phys. Lett.* **93,** 252502 (2008).
29. Olejník, K. *et al.* Enhanced annealing, high Curie temperature and low-voltage gating in (Ga,Mn)As: a surface oxide control study. *Phys. Rev. B* **78,** 054403 (2008).
30. Wang, M. *et al.* Achieving high Curie temperature in (Ga,Mn)As. *Appl. Phys. Lett.* **93,** 132103 (2008).
31. Chen, L. *et al.* Low-temperature magnetotransport behaviors of heavily Mn-doped (Ga,Mn)As films with high ferromagnetic transition temperature. *Appl. Phys. Lett.* **95,** 182505 (2009).
32. Akai, H. Ferromagnetism and its stability in the diluted magnetic semiconductor (In,Mn)As. *Phys. Rev. Lett.* **81,** 3002–3005 (1998).
33. Sato, K., Dederichs, P. H. & Katayama-Yoshida, H. Curie temperatures of III-V diluted magnetic semiconductors calculated from first principles. *Europhys. Lett.* **61,** 403–408 (2003).
34. Mahadevan, P. & Zunger, A. Trends in ferromagnetism, hole localization, and acceptor level depth for Mn substitution in GaN, GaP, GaAs, GaSb. *Appl. Phys. Lett.* **85,** 2860–2862 (2004).
35. Burch, K., Awschalom, D. & Basov, D. Optical properties of III-Mn-V ferromagnetic semiconductors. *J. Magn. Magn. Mater.* **320,** 3207–3228 (2008).
36. Alberi, K. *et al.* Formation of Mn-derived impurity band in III-Mn-V alloys by valence band anticrossing. *Phys. Rev. B* **78,** 075201 (2008).
37. Liu, C., Yun, F. & Morkoç, H. Ferromagnetism of ZnO and GaN: a review. *J. Mater. Sci. Mater. Electron.* **16,** 555–597 (2005).
38. Coey, J. M. D. Dilute magnetic oxides. *Curr. Opin. Solid State Mater. Sci.* **10,** 83–92 (2006).
39. Bonanni, A. Ferromagnetic nitride-based semiconductors doped with transition metals and rare earths. *Semicond. Sci. Technol.* **22,** R41–R56 (2007).
40. Sato, K. *et al.* First-principles theory of dilute magnetic semiconductors. *Rev. Mod. Phys.* **82,** 1633–1690 (2010).
41. Blinowski, J., Kacman, P. & Majewski, J. A. Ferromagnetic superexchange in Cr-based diluted magnetic semiconductors. *Phys. Rev. B* **53,** 9524–9527 (1996).
42. Walsh, A., Da Silva, J. L. F. & Wei, S-H. Theoretical description of carrier mediated magnetism in cobalt doped ZnO. *Phys. Rev. Lett.* **100,** 256401 (2008).
43. Coey, J. M. D., Venkatesan, M. & Fitzgerald, C. B. Donor impurity band exchange in dilute ferromagnetic oxides. *Nature Mater.* **4,** 173–179 (2005).
44. Wang, Q., Sun, Q., Jena, P. & Kawazoe, Y. Magnetic properties of transition-metal-doped $Zn_{1-x}T_xO$ (T = Cr, Mn, Fe, Co, and Ni) thin films with and without intrinsic defects: a density functional study. *Phys. Rev. B* **79,** 115407 (2009).
45. Park, C. H. & Chadi, D. J. Hydrogen-mediated spin-spin interaction in ZnCoO. *Phys. Rev. Lett.* **94,** 127204 (2005).
46. Coey, J. M. D., Wongsaprom, K., Alaria, J. & Venkatesan, M. Charge-transfer ferromagnetism in oxide nanoparticles. *J. Phys. D* **41,** 134012 (2008).
47. Dietl, T. Dilute magnetic semiconductors: functional ferromagnets. *Nature Mater.* **2,** 646–648 (2003).
48. Cho, Y. J., Yu, K. M., Liu, X., Walukiewicz, W. & Furdyna, J. K. Effects of donor doping on $Ga_{1-x}Mn_xAs$. *Appl. Phys. Lett.* **93,** 262505 (2008).
49. Mayer, M. A. *et al.* Electronic structure of $Ga_{1-x}Mn_xAs$ analyzed according to hole-concentration-dependent measurements. *Phys. Rev. B* **81,** 045205 (2010).
50. Jungwirth, T. *et al.* Character of states near the Fermi level in (Ga,Mn)As: impurity to valence band crossover. *Phys. Rev. B* **76,** 125206 (2007).
51. Dietl, T. Interplay between carrier localization and magnetism in diluted magnetic and ferromagnetic semiconductors. *J. Phys. Soc. Jpn* **77,** 031005 (2008).
52. Altshuler, B. L. & Aronov, A. G. in *Electron-Electron Interactions in Disordered Systems* (eds Efros, A. L. & Pollak, M.) 1–153 (North Holland, 1985).
53. Lee, P. A. & Ramakrishnan, T. V. Disordered electronic systems. *Rev. Mod. Phys.* **57,** 287–337 (1985).
54. Belitz, D. & Kirkpatrick, T. R. The Anderson-Mott transition. *Rev. Mod. Phys.* **66,** 261–380 (1994).
55. Edwards, P. P. & Sienko, M. J. Universality aspects of the metal-nonmetal transition in condensed media. *Phys. Rev. B* **17,** 2575–2581 (1978).
56. Dietl, T., Matsukura, F. & Ohno, H. Ferromagnetism of magnetic semiconductors: Zhang-Rice limit. *Phys. Rev. B* **66,** 033203 (2002).
57. Dietl, T. Hole states in wide band-gap diluted magnetic semiconductors and oxides. *Phys. Rev. B* **77,** 085208 (2008).
58. Neumaier, D. *et al.* All-electrical measurement of the density of states in (Ga,Mn)As. *Phys. Rev. Lett.* **103,** 087203 (2009).
59. Boukari, H. *et al.* Light and electric field control of ferromagnetism in magnetic quantum structures. *Phys. Rev. Lett.* **88,** 207204 (2002).
60. Nishitani, Y. *et al.* Curie temperature versus hole concentration in field-effect structures of $Ga_{1-x}Mn_xAs$. *Phys. Rev. B* **81,** 045208 (2010).
61. MacDonald, A. H., Schiffer, P. & Samarth, N. Ferromagnetic semiconductors: moving beyond (Ga,Mn)As. *Nature Mater.* **4,** 195–202 (2005).
62. Edmonds, K. W. *et al.* High Curie temperature GaMnAs obtained by resistance-monitored annealing. *Appl. Phys. Lett.* **81,** 4991–4993 (2002).
63. Cho, Y. J., Liu, X. & Furdyna, J. K. Collapse of ferromagnetism in (Ga,Mn)As at high hole concentrations. *Semicond. Sci. Technol.* **23,** 125010 (2008).
64. Furdyna, J. K. *et al.* Fermi level effects on Mn incorporation in modulation-doped ferromagnetic $III_{1-x}Mn_xV$ heterostructures. *J. Phys. Condens. Matter* **16,** S5499–S5508 (2004).
65. Scarpulla, M. A. *et al.* Ferromagnetism in $Ga_{1-x}Mn_xP$: evidence for inter-Mn exchange mediated by localized holes within a detached impurity band. *Phys. Rev. Lett.* **95,** 207204 (2005).
66. Schallenberg, T. & Munekata, H. Preparation of ferromagnetic (In,Mn)As with a high Curie temperature of 90 K. *Appl. Phys. Lett.* **89,** 042507 (2006).
67. Abe, E., Matsukura, F., Yasuda, H., Ohno, Y. & Ohno, H. Molecular beam epitaxy of III-V diluted magnetic semiconductor (Ga,Mn)Sb. *Physica E* **7,** 981–985 (2000).
68. Wojtowicz, T. *et al.* $In_{1-x}Mn_xSb$ — a new narrow gap ferromagnetic semiconductor. *Appl. Phys. Lett.* **82,** 4310–4312 (2003).
69. Jungwirth, T., König, J., Sinova, J., Kučera, J. & MacDonald, A. H. Curie temperature trends in (III,Mn)V ferromagnetic semiconductors. *Phys. Rev. B* **66,** 012402 (2002).

70. Jungwirth, T., Sinova, J., Mašek, J., Kučera, J. & MacDonald, A. H. Theory of ferromagnetic (III,Mn)V semiconductors. *Rev. Mod. Phys.* **78,** 809–864 (2006).
71. Glunk, M. *et al.* Magnetic anisotropy in (Ga,Mn)As: influence of epitaxial strain and hole concentration. *Phys. Rev. B* **79,** 195206 (2009).
72. Kodzuka, M., Ohkubo, T., Hono, K., Matsukura, F. & Ohno, H. 3DAP analysis of (Ga,Mn)As diluted magnetic semiconductor thin film. *Ultramicroscopy* **109,** 644–648 (2009).
73. Yu, K. M. *et al.* Effect of the location of Mn sites in ferromagnetic $Ga_{1-x}Mn_xAs$ on its Curie temperature. *Phys. Rev. B* **65,** 201303 (2002).
74. Wierzbowska, M., Sanchez-Portal, D. & Sanvito, S. Different origin of the ferromagnetic order in (Ga,Mn)As and (Ga,Mn)N. *Phys. Rev. B* **70,** 235209 (2004).
75. Schulthess, T., Temmerman, W. M., Szotek, Z., Butler, W. H. & Stocks, G. M. Electronic structure and exchange coupling of Mn impurities in III-V semiconductors. *Nature Mater.* **4,** 838–844 (2005).
76. Kitchen, D., Richardella, A., Tang, J-M., Flatte, M. E. & Yazdani, A. Atom-by-atom substitution of Mn in GaAs and visualization of their hole-mediated interactions. *Nature* **442,** 436–439 (2006).
77. Sarigiannidou, E. *et al.* Intrinsic ferromagnetism in wurtzite (Ga,Mn)N semiconductor. *Phys. Rev. B* **74,** 041306 (2006).
78. Martinez-Criado, G. *et al.* Mn-rich clusters in GaN: hexagonal or cubic symmetry? *Appl. Phys. Lett.* **86,** 131927 (2005).
79. Lipińska, A. *et al.* Ferromagnetic properties of p-(Cd,Mn)Te quantum wells: interpretation of magneto-optical measurements by Monte Carlo simulations. *Phys. Rev. B* **79,** 235322 (2009).
80. Ferrand, D. *et al.* Carrier-induced ferromagnetism in p-$Zn_{1-x}Mn_xTe$. *Phys. Rev. B* **63,** 085201 (2001).
81. Andrearczyk, T. *et al.* in *Proc. 25th Int. Conf. Phys. Semicond.* (eds Miura, N. & Ando, T.) 234–235 (Springer, 2001).
82. Serrate, D., Teresa, J. M. D. & Ibarra, M. R. Double perovskites with ferromagnetism above room temperature. *J. Phys. Condens. Matter* **19,** 023201 (2007).
83. Park, J. H., Kim, M. G., Jang, H. M., Ryu, S. & Kim, Y. M. Co-metal clustering as the origin of ferromagnetism in Co-doped ZnO thin films. *Appl. Phys. Lett.* **84,** 1338–1340 (2004).
84. Ney, A. *et al.* Advanced spectroscopic synchrotron techniques to unravel the intrinsic properties of dilute magnetic oxides: the case of Co:ZnO. *N. J. Phys.* **12,** 013020 (2010).
85. Bonanni, A. *et al.* Paramagnetic GaN:Fe and ferromagnetic (Ga,Fe)N: the relationship between structural, electronic, and magnetic properties. *Phys. Rev. B* **75,** 125210 (2007).
86. Boeck, J. D. *et al.* Nanometer-scale magnetic MnAs particles in GaAs grown by molecular beam epitaxy. *Appl. Phys. Lett.* **68,** 2744–2746 (1996).
87. Moreno, M., Trampert, A., Jenichen, B., Däweritz, L. & Ploog, K. H. Correlation of structure and magnetism in GaAs with embedded Mn(Ga)As magnetic nanoclusters. *J. Appl. Phys.* **92,** 4672–4677 (2002).
88. Rovezzi, M. *et al.* Local structure of (Ga,Fe)N and (Ga,Fe)N:Si investigated by X-ray absorption fine structure spectroscopy. *Phys. Rev. B* **79,** 195209 (2009).
89. Bonanni, A. *et al.* Controlled aggregation of magnetic ions in a semiconductor: an experimental demonstration. *Phys. Rev. Lett.* **101,** 135502 (2008).
90. Tanaka, M., Yokoyama, M., Hai, P. N. & Ohya, S. in *Spintronics* (eds Dietl, T., Awschalom, D. D., Kaminska, M. & Ohno, H.) 455–485 (Semiconductors and Semimetals 82, Elsevier, 2008).
91. Kuroda, S. *et al.* Origin and control of high temperature ferromagnetism in semiconductors. *Nature Mater.* **6,** 440–446 (2007).
92. Gu, L. *et al.* Characterization of Al(Cr)N and Ga(Cr)N dilute magnetic semiconductors. *J. Magn. Magn. Mater.* **290–291,** 1395–1397 (2005).
93. Jamet, M. *et al.* High-Curie-temperature ferromagnetism in self-organized $Ge_{1-x}Mn_x$ nanocolumns. *Nature Mater.* **5,** 653–659 (2006).
94. Nishio, Y., Ishikawa, K., Kuroda, S., Mitome, M. & Bando, Y. in *Mater. Res. Soc. Symp. Proc.* Vol. 1183-FF01-11 (Materials Research Society, 2009).
95. Katayama-Yoshida, H. *et al.* Theory of ferromagnetic semiconductors. *Phys. Status Solidi A* **204,** 15–32 (2007).
96. Dietl, T. Self-organised growth controlled by charge states of magnetic impurities. *Nature Mater.* **5,** 673 (2006).
97. Ye, L-H. & Freeman, A. J. Defect compensation, clustering, and magnetism in Cr-doped anatase. *Phys. Rev. B* **73,** 081304(R) (2006).
98. Straumal, B. B. *et al.* Magnetization study of nanograined pure and Mn-doped ZnO films: formation of a ferromagnetic grain-boundary foam. *Phys. Rev. B* **79,** 205206 (2009).
99. Ney, A. *et al.* Absence of intrinsic ferromagnetic interactions of isolated and paired Co dopant atoms in $Zn_{1-x}Co_xO$ with high structural perfection. *Phys. Rev. Lett.* **100,** 157201 (2008).
100. van Schilfgaarde, M. & Mryasov, O. N. Anomalous exchange interactions in III-V dilute magnetic semiconductors. *Phys. Rev. B* **63,** 233205 (2001).
101. Zunger, A. in *Solid State Physics* Vol. 39 (eds Seitz, F. & Turnbull, D.) 275–464 (Academic, 1986).
102. Furdyna, J. K. & Kossut, J. (eds) *Diluted Magnetic Semiconductors* (Semiconductors and Semimetals 25, Academic, 1988).
103. Da Silva, J. L. F., Dalpian, G. M. & Wei, S-H. Carrier-induced enhancement and suppression of ferromagnetism in $Zn_{1-x}Cr_xTe$ and $Ga_{1-x}Cr_xAs$: origin of the spinodal decomposition. *N. J. Phys.* **10,** 113007 (2008).
104. Hai, P. N., Ohya, S., Tanaka, M., Barnes, S. E. & Maekawa, S. Electromotive force and huge magnetoresistance in magnetic tunnel junctions. *Nature* **458,** 489–492 (2007).
105. Katayama-Yoshida, H., Sato, K., Fukushima, T. & Toyoda, M. H. K. & Dinh, V. A. in *Spintronics* (eds Dietl, T., Awschalom, D. D., Kaminska, M. & Ohno, H.) 433–454 (Semiconductors and Semimetals 82, Elsevier, 2008).
106. Geshi, M., Kusakabe, K., Tsukamoto, H. & Suzuki, N. A new ferromagnetic material excluding transition metals: CaAs in a distorted zinc-blende structure. *AIP Conf. Proc.* **772,** 327–328 (2005).
107. Volnianska, O. & Boguslawski, P. Magnetism of solids resulting from spin polarization of *p* orbitals. *J. Phys. Condens. Matter* **22,** 073202 (2010).
108. Elfimov, I. S., Yunoki, S. & Sawatzky, G. A. Possible path to a new class of ferromagnetic and half-metallic ferromagnetic materials. *Phys. Rev. Lett.* **89,** 216403 (2002).
109. Sliwa, C. & Dietl, T. Electron-hole contribution to the apparent *s-d* exchange interaction in III-V dilute magnetic semiconductors. *Phys. Rev. B* **78,** 165205 (2008).
110. Grace, P. J. *et al.* The origin of the magnetism of etched silicon. *Adv. Mater.* **21,** 71–74 (2009).
111. Sperl, M. *et al.* Identifying the character of ferromagnetic Mn in epitaxial Fe/(Ga,Mn)As heterostructures. *Phys. Rev. B* **81,** 035211 (2010).
112. Shick, A. B., Khmelevskyi, S., Mryasov, O. N., Wunderlich, J. & Jungwirth, T. Spin-orbit coupling induced anisotropy effects in bimetallic antiferromagnets: a route towards antiferromagnetic spintronics. *Phys. Rev. B* **81,** 212409 (2010).


## Acknowledgements

This work was supported by the FunDMS Advanced Grant of the European Research Council within the 'Ideas' 7th Framework Programme of the EC, and earlier by the ERATO project of the Japan Science and Technology Agency and the Alexander von Humboldt Foundation. Collaboration with the groups of A. Bonanni, S. Kuroda, H. Ohno and M. Sawicki is gratefully acknowledged.